University of Essex

Theory of electron transport in dilute GaAs:N

School of Computer Science and Electronic Engineering

M. P. Vaughan and B.K. Ridley

Optoelectronics Research Group, University of Essex, Colchester, CO4 3SQ

Abstract

Using an *n*-level generalisation of the band anticrossing (BAC) model [1-6], the essential features of the non-parabolicity of the band structure in dilute nitride materials can be captured using a **k.p** – like formulation. However, the derived densities of states in both 3D and 2D are then badly behaved near the nitrogen impurity levels with unrealistic consequences. Densities of states are derived [5,6] from the Green's function of the Anderson many-impurity model [7], which are well-behaved and conserve the number of states in the crystal.

The scattering rate is derived [5,6] from the Hamiltonian using an *S*-matrix approach and the nitrogen scattering limited mobility calculated for bulk and 2D.

The densities of states

The non-parabolicity can be described by defining*

$$\gamma(E) = \frac{\hbar^2 k^2}{2m^*} = \sum_j \frac{\beta_j^2 x_j}{E_j - E} + E, \qquad (1)$$

In the general case of finite energy broadening on the N states, we define

$$\Omega(E) = -\sum_j \Omega_j(E), \quad \Omega_j(E) = \frac{\beta_j^2 x_j \Delta_j}{(E - E_j)^2 + \Delta_j^2}$$

and

$$\Gamma(E) = E - \sum_j \frac{(E - E_j)}{\Delta_j} \Omega_j(E), \qquad (2)$$

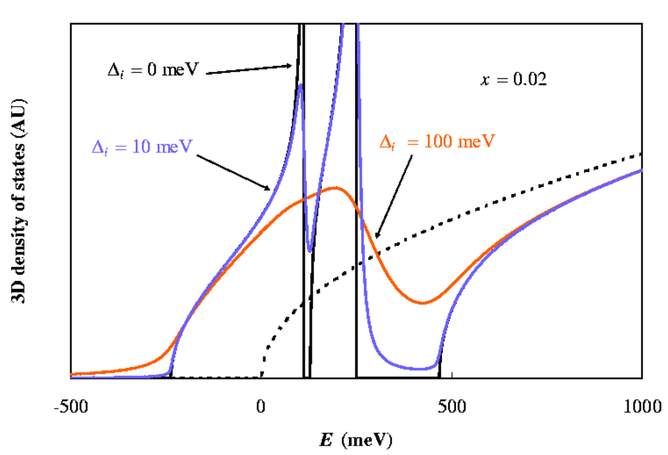

Figure 1 The 3D density of states for a 3-band model with different energy broadenings on the *N* states. The dotted line shows the matrix semiconductor density of states.

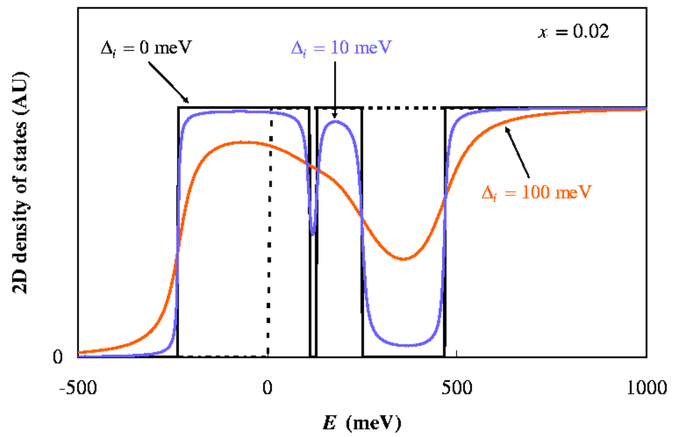

Figure 2 The 2D density of states for a 3 band model in a single subband for different energy broadenings. The dotted line shows the density of states of the matrix semiconductor.

The densities of states are*

$$N_{3D}(E) = -\frac{(2m^*)^{3/2}}{4\pi^2\hbar^3} \Omega(E) \left\{ 2\left[\left(\Gamma^2(E) + \Omega^2(E) \right)^{1/2} - \Gamma(E) \right] \right\}^{-1/2} \qquad (3)$$

and

$$N_{2D}(E) = \frac{m^*}{2\pi\hbar^2} \sum_n \left\{ \frac{1}{2} - \frac{1}{\pi} \arctan\left(\frac{\Gamma(E) - E_n}{\Omega(E)} \right) \right\}. \qquad (4)$$

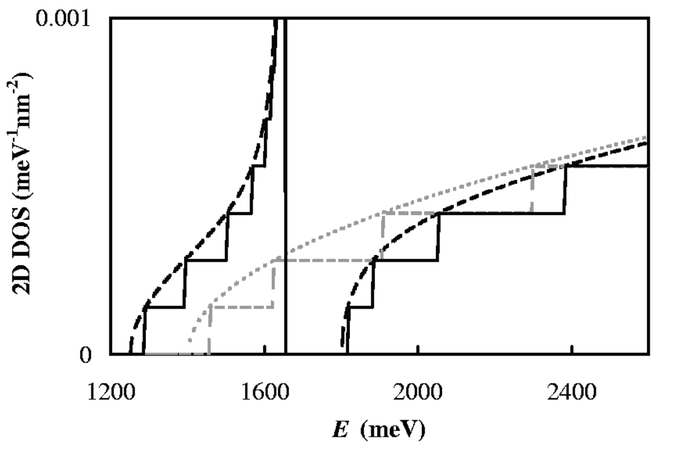

Figure 3 The 2D density of states for a 2-band model summed over sub-bands for zero energy broadening. The dotted line shows the density of states of the matrix semiconductor.

In the limit as $\Delta_j \to 0$, we have

$$\lim_{\Delta_j \to 0} N_{3D}(E) = \frac{(2m^*)^{3/2}}{4\pi^2\hbar^3} \gamma^{1/2}(E). \qquad (5)$$

and

$$\lim_{\Delta_j \to 0} N_{2D}(E) = \frac{m^*}{2\pi\hbar^2} \sum_n \theta[\gamma(E) - E_n]. \qquad (6)$$

In general case, we find

$$\lim_{\Delta_j \to 0} N(E) = N_0\{\gamma(E)\}, \qquad (7)$$

where $N_0(E)$ is the density of states of the matrix semiconductor.

The relaxation time

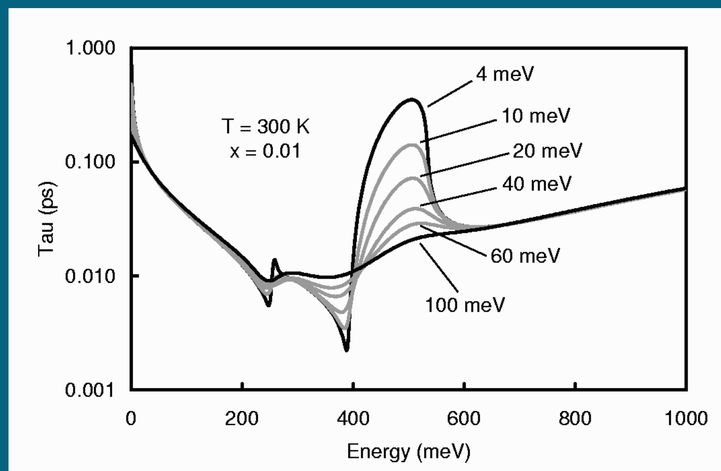

Figure 4 The relaxation time calculated for a 3-band model in 3D for different energy broadenings. The peaks occur in the energy gaps due to the vanishing DOS there.

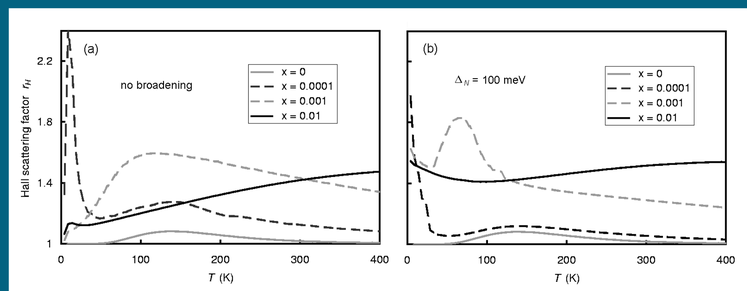

Figure 5 Since the Hall scattering factor $r_H = 1 + \mathrm{var}(\tau)/\langle\tau\rangle^2$, the large variation in the relaxation time leads to an enhancement of r_H. Calculations incorporate LO and acoustic phonon scattering with magnetic field $B = 0.5$ T

3D Mobility

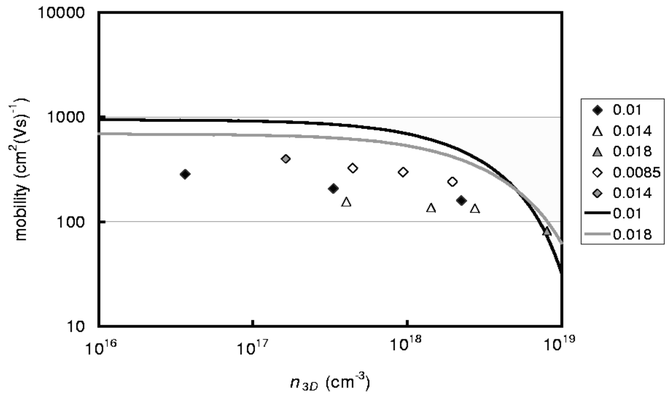

Figure 6 Calculated and measured mobility as a function of carrier density at different nitrogen concentrations. Data points are from reference [8].

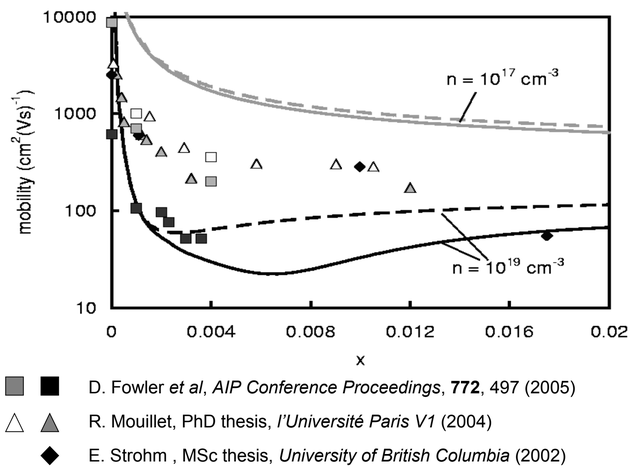

Figure 7 Calculated and measured mobilities as a function of nitrogen concentration at different carrier densities.

3D Mobility

In Figure 6, we show calculated mobilities using degenerate statistics in comparison to measurements of quantum well structures by Mouillet [8] At most carrier concentrations, the calculated values are an overestimate. The drop in mobility at higher carrier concentration is due to the Fermi energy being pushed higher into the band where the fractional Γ character, and hence the group velocity, is reduced.

Fig. 9 shows the calculated mobility as a function of nitrogen concentration in comparison to measurements by Mouillet [8], Fowler *et al* [9], and Strohm [10]. The Se-doped samples were reported by Fowler et al to exhibit very high carrier concentrations (~10^{19} cm^{-3}) and here the fit with either the 2-band (dashed line) or 3-band (solid line) is good at the measured nitrogen concentrations. Note that the dip in the 3-band model curve at around x = 0.006 absent from the 2-band calculations is due to the Fermi energy becoming coincident with the N-N pair energy, where the fractional Γ character is severely reduced. In the measurements by Mouillet, a range of carrier concentrations were found from 5 × 10^{16} cm^{-3} – 2.5 × 10^{17} cm^{-3}, decreasing with x. The calculated mobilities at 10^{17} cm^{-3} are once again an overestimate.

2D Mobility

Figure 8 shows the calculation of the mobility as a function of well width d at different carrier concentrations for the 3 band model with T = 300 K and N fraction x = 0.01. As with bulk calculations, the mobility decreases dramatically at high carrier concentrations. Additionally, we see that for d < ~15 nm, the mobility drops off with well width. The cause of this drop in mobility is related in both cases: The increase in n_{3D} pushes the Fermi energy up towards the isolated N energy where both the scattering is increased and the group velocity becomes small. Similarly, decreasing d pushes up the subband energies with the same consequence. The calculations for the 2 band model are qualitatively similar but give slightly higher mobilities.

Figure 9 shows a comparison of calculated mobility as a function of N content against experimental measurements by Fowler *et al* [9]. The white and grey circles are calculations for d = 13 nm corresponding to a modulation-doped and directly (Si) doped quantum well. The difference in these calculations arises purely out of the difference in carrier density, no account of ionised impurity scattering being incorporated in the latter case. The black circles are for a highly degenerate (n_{3D} ~ 10^{19} cm^{-3}) 100 nm well. At such a width, the mobility would be bulk-like and the low values are purely due to the high carrier concentration. In fact, calculations for n_{3D} = 10^{19} cm^{-3} give even lower results than those shown and here we have used n_{3D} = 8 × 10^{18} cm^{-3}.

***Symbols used in expressions**

β_j	interaction strength of the jth N impurity type
x_j	concentration of the jth N impurity type
E_j	energy of the jth N impurity type
Δ_j	energy broadening on the jth N impurity type
E_n	energy at the bottom of the nth subband

2D Mobility

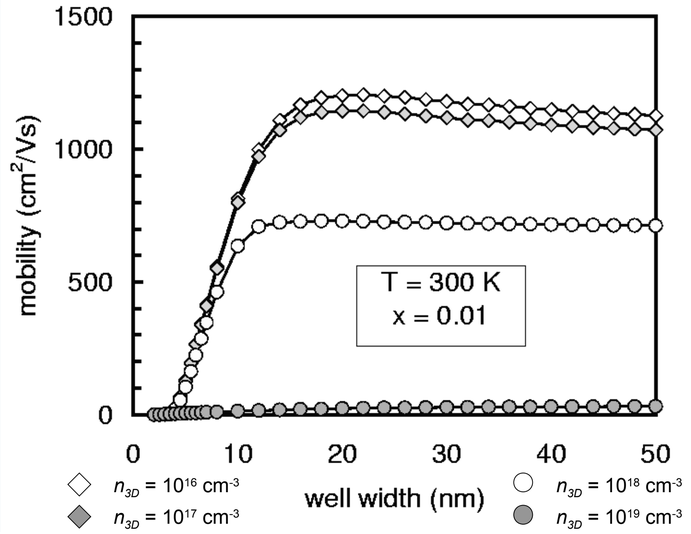

Figure 8 Calculated 2D mobility as a function of well width for different carrier densities.

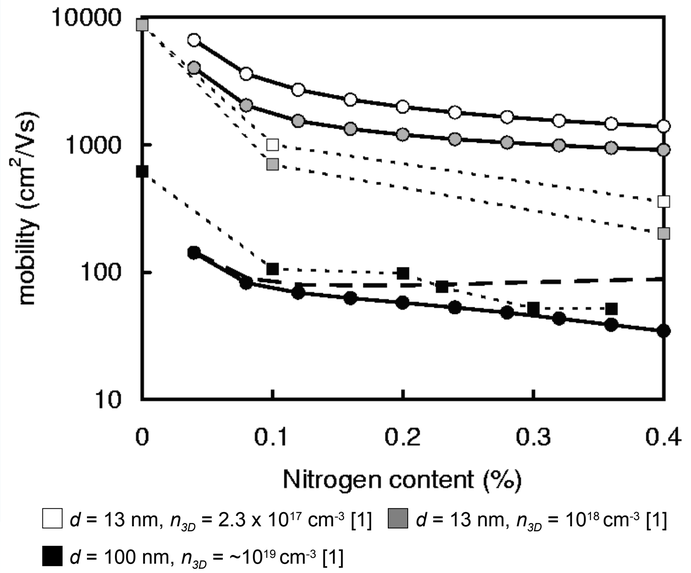

Figure 9 Calculated and measured 2D mobilities as a function of nitrogen concentration at different carrier densities. Circles are calculated mobilities (3-band model). Dashed line is 2-band model. Measured data is from reference [9].

References

[1] W. Shan *et al*, *Phys. Rev. Lett*., **82**, p. 1221, (1999)

[2] A. Lindsay, PhD Thesis, University of Surrey, (2002)

[3] S. Fahy and E.P. O'Reilly, *Physica E*, 21, p. 881 (2004)

[4] S.B. Healy, A. Lindsay and E.P. O'Reilly, *IEE Proc.-Optoelectron*., 151, p. 397 (2004)

[5] M.P. Vaughan and B.K. Ridley, *Phys. Rev. B*, **75**, 195205 (2007)

[6] M.P. Vaughan, *Alloy and Phonon Scattering: Development of Theoretical Models for Dilute Nitrides*, VDM Verlag Dr. Müller (2009)

[7] P.W. Anderson, *Phys. Rev*., **124**, p. 41 (1961)

[8] R. Mouillet, PhD thesis, l'Université Paris V1 (2004)

[9] D. Fowler et al, AIP Conference Proceedings, **772**, 497 (2005)

[10] E. Strohm , MSc thesis, University of British Columbia (2002)

Acknowledgements

This work has been support by a grant from the Engineering and Physical Sciences Research Council.

Website: http://privatewww.essex.ac.uk/~mpvaug/

Contact: mpvaug@essex.ac.uk